ANTIOXIDANTS & REDOX SIGNALING
Volume 7, Numbers 3 & 4, 2005

Forum Original Research Communication

Antiapoptotic Response to Induced GSH Depletion: Involvement of Heat Shock Proteins and NF-κB Activation

GIUSEPPE FILOMENI, KATIA AQUILANO, GIUSEPPE ROTILIO, and MARIA R. CIRIOLO

ABSTRACT

Alteration of glutathione (GSH) homeostasis represents one of the earliest events during the commitment of stress-induced apoptosis. Extrusion of GSH into the extracellular milieu, in response to several oxidative stimuli, has been suggested as a molecular switch triggering apoptosis. However, chemical depletion of GSH does not induce cell death even though cytochrome *c* release from mitochondria has been observed. Here we report that U937 cells treated with buthionine sulfoximine (BSO) are able to survive and to inhibit the apoptotic program downstream of cytochrome *c* release. BSO treatment induces a highly significant decrease of GSH in both the cytosolic and mitochondrial fractions. The concomitant release of cytochrome *c* into the cytosol was associated with nuclear translocation of apoptosis-inducing factor. GSH depletion also resulted in reactive oxygen species production and in a specific increase of mitochondrial protein carbonyls. However, all these events were transiently present inside cells and efficiently counteracted by cell-repairing systems. We observed an increase in the proteasome activity and in the expression levels of heat shock protein 27 (Hsp27) and Hsp70. Moreover, nuclear factor-κB (NF-κB) was activated in our system as a survival cell response against the oxidative injury. Overall results suggest that activation of NF-κB and Hsp could allow cell adaptation and survival under exhaustive GSH depletion. *Antioxid. Redox Signal.* 7, 446–455.

INTRODUCTION

THE APOPTOTIC PATHWAY activated by chemical or physical stresses such as ultraviolet and γ radiations, growth factor withdrawal, and prooxidant molecules has been defined as the "mitochondrial pathway" because these organelles are the place where well characterized and crucial events for commitment of apoptosis occur. Particularly, cytochrome *c* release into the cytosol is the primary event for the formation of the apoptosome, a multimolecular complex that mediates the activation of the upstream cysteine protease (caspase-9), which in turn proteolyzes and activates the executioner downstream caspases (caspase-3, -6, and -7) (5, 31). Cytochrome *c* can be released from the intermembrane space into the cytosol through pores formed by specialized proteins such as Bax, a proapoptotic member of the Bcl-2 superfamily (22), or by the opening of existing pores functioning within the energy metabolism (18).

Moreover, other proapoptotic factors are resident in mitochondria. Smac (second mitochondria-derived activator of caspases) and its murine homologue DIABLO (direct IAP-binding protein with low pI) have been described to bind specific inhibitors of apoptotic proteins (IAPs) in order to induce programmed cell death (1). The interactions between cytosolic (IAPs) and mitochondrial (Smac/DIABLO, cytochrome *c*) proteins modulate caspase activation, which in turn can induce or inhibit apoptosis. Apoptosis-inducing factor (AIF), a flavoprotein with oxidoreductase function, can be released also in response to apoptotic stimuli, and upon translocation into the nucleus it can induce caspase-independent apoptotic cell death (6).

Mitochondria are also the main source of reactive oxygen species (ROS) as by-product of oxygen consumption either under physiological conditions or as secondary effect of apoptosis execution. In particular, several apoptotic inducers are prooxidant agents, and various proteins and apoptotic pathways

Department of Biology, University of Rome "Tor Vergata," Rome, Italy.

are inhibited by antioxidants, as well as by overexpression of the antiapoptotic protein Bcl-2 by way of the antioxidant pathway (19). Among different antioxidant systems operative in the cell in order to buffer the ROS-mediated oxidative damage, glutathione (GSH) represents the most important low-molecular-weight antioxidant (8); it participates in reactions normally opposed to ROS production, *e.g.,* that catalyzed by glutathione peroxidase (10). Moreover, different apoptotic agents induce an early active extrusion of GSH from cells leading to widespread mitochondrial damage and to cytochrome *c* release from the intermembrane space into the cytosol (11, 14). However, the latter process was not directly related to induction of the apoptotic process because cell viability, in several experimental systems, was not affected when the depletion of the tripeptide was obtained by chemical inhibition of its synthesis (16).

Heat shock proteins (Hsps) have recently been found to interact negatively with the apoptotic mitochondrial machinery. It has been demonstrated that Hsp70 has the capability to interact and recruit apoptosis protease-activating factor 1 (Apaf1) and to antagonize AIF (26, 30), whereas Hsp27 can bind cytochrome *c* in order to prevent apoptosome oligomerization and activation (4). Hsps are ubiquitous and highly conserved proteins whose expression is induced in response to a wide variety of physiological and stress insults (13); they act as molecular chaperones by helping the refolding of misfolded proteins and assisting their elimination when they become irreversibly damaged. Hsp synthesis is tightly regulated at the transcriptional level by heat shock factors (HSFs). Although various HSFs were reported, HSF1 was shown to be the main regulator of the short-term induction. Under resting conditions, HSF1 is found to be associated with the inhibitory subunits Hsp90 and Hsp70. Upon chemical or physical insults, such as heat shock or oxidative stress, incorrectly folded proteins recruit Hsp90 and Hsp70, leaving HSF1 free to trimerize, autophosphorylate, and translocate into the nucleus where it activates *hsp* gene transcription (25). The antiapoptotic action of Hsps is also mediated by the interaction of specific isoforms with proteins that generate a survival signal in response to different stimuli (24). For instance, Hsp90 interacts with and stabilizes RIP-1 kinase and serine threonine kinase (Akt/protein kinase B), proteins that connect death receptors or growth factor stimulation to nuclear factor-κB (NF-κB) activation (20). NF-κB is important for the expression of a wide variety of genes that are involved in cell proliferation and survival. In unstimulated cells, NF-κB is predominantly localized in the cytoplasm and is associated with the inhibitory protein IκB. The several steps of activation of this nuclear factor involve the ubiquitin/proteasome system, including maturation of the transcription factor subunits, activation of IκB kinases, and degradation of IκB (20). In fact, upon cell stimulation, a specific IκB protein kinase catalyzes the phosphorylative modification of IκB, thus targeting it for a rapid degradation via the ubiquitin/proteasome pathway and leaving NF-κB free to translocate into the nucleus where it transactivates transcription of target genes (17). It has also been reported that Hsp27 facilitates phosphorylated and ubiquitylated IκB proteolytic degradation (24). The mitochondrial cell death pathway seems to be profoundly affected by Hsp especially when the inducer of apoptosis is a stress-related factor.

To explore directly the role of GSH in the induction of apoptosis, we have investigated the effects of GSH depletion in U937 cells. Here we report that treatment with buthionine sulfoximine (BSO), a specific inhibitor of GSH synthesis, induced a time-dependent loss of the tripeptide. This decrease was associated with an efficient release of cytochrome *c* into the cytosol, nuclear translocation of AIF, and increased ROS production without significant commitment to cell death at longer time points. An increase of the Hsp70 and Hsp27 expression levels, in addition to HSF1 activation, efficiently buffered the events downstream of GSH depletion. NF-κB induction was also observed, thus cooperating in allowing cell survival under oxidative conditions.

MATERIALS AND METHODS

Cell cultures, treatments, and determination of cell death

Human promonocytic cell line U937 and T-cell leukemia cell line CEM were purchased from European Type Culture Collection and grown in RPMI 1640 medium supplemented with 10% fetal bovine serum at 37°C in an atmosphere containing 5% CO_2. Cells were routinely collected by centrifugation at 700 *g* and resuspended in fresh medium at a concentration of 2×10^5/ml.

BSO (Sigma Chemical Co., St. Louis, MO, U.S.A.), a specific inhibitor of γ-glutamylcysteine synthetase, was added in culture medium at a concentration of 1 m*M*.

Puromycin (Sigma), a well characterized aminonucleoside antibiotic and apoptotic inducer, was prepared just before the experiments and used at a concentration of 10 μ*M* for 6 h.

Cell viability was assessed by trypan blue exclusion. Alternatively, cells were washed in phosphate-buffered saline (PBS), stained with 50 μg/ml propidium iodide, and analyzed by a FACScalibur instrument (Becton Dickinson, San Jose, CA, U.S.A.). The percentages of apoptotic cells were evaluated according to Nicoletti *et al.* (23) by calculating peak area of hypodiploid nuclei.

GSH determination and other assays

Intracellular GSH was assayed upon formation of *S*-carboxymethyl derivatives of free thiols with iodoacetic acid, followed by the conversion of free amino groups to 2,4-dinitrophenyl derivatives by the reaction with 1-fluoro-2,4-dinitrobenzene as described by Reed *et al.* (27). Cell suspension was washed three times with PBS, resuspended, and lysed by repeated cycles of freezing and thawing under liquid nitrogen. Lysates were then utilized for GSH/GSSG assay prior to derivatization, as described previously (9). Data are expressed as nanomoles of GSH per milligram of protein.

Measurement of intracellular ROS

U937 cells were incubated in culture medium with 5 μ*M* dihydrorhodamine 123 (DHR 123) (Molecular Probes, Eugene, OR, U.S.A.) for 30 min at 37°C, pelletted, washed, and resuspended in ice-cold PBS. The fluorescence intensities of hydrorhodamine 123, formed by the reaction of DHR 123

with ROS, of >10,000 cells from each sample, were analyzed by recording FL-2 fluorescence by a flow cytometer. Experiments were repeated at least three times with similar results. The data are given as one representative histogram.

Cell fractionation and protein extraction

Total protein extracts were obtained by disrupting cells with 30 min of incubation on ice in lysis buffer containing 50 m*M* Tris-HCl, pH 7.4, 1 m*M* EDTA, 1 m*M* EGTA, 0.1% Triton X-100, and protease inhibitor cocktail (Sigma). Supernatants obtained after centrifugation at 22,300 *g* for 20 min were used for the experiments.

Cell fractions were obtained by incubating in ice 9×10^6 cells in 0.2 ml of a hypotonic medium containing 10 m*M* Tris-HCl, pH 7.5, 15 m*M* $MgCl_2$, 10 m*M* KCl, and protease inhibitor cocktail. After 10 min on ice, equal volumes of a "mitochondrial" buffer containing 400 m*M* sucrose, 10 m*M* TES, 0.1 m*M* EGTA, and 2 μ*M* dithiothreitol, pH 7.2, was added, and cells were disrupted by 40 strokes in a glass Dounce. Pellets, obtained after centrifugation of lysates at 900 *g* for 10 min, were considered as nuclear-enriched fractions. Mitochondria-containing supernatants were further centrifuged at 10,000 *g* for 15 min to finally separate organelles (pellet) from the cytosolic enriched fraction (super). For protein determination, mitochondria and nuclei were lysed in lysis buffer.

Immunoblots

Proteins were boiled in sodium dodecyl sulfate (SDS)-containing sample buffer, electrophoresed on SDS-polyacrylamide gels, and blotted onto nitrocellulose membranes. Membranes were stained with primary antibodies, and after incubation with the appropriate horseradish peroxidase-conjugated secondary antibodies, immunoreactive bands were detected by an enhanced chemiluminescence kit (Pierce, Rockford, IL, U.S.A.). The primary antibodies used were monoclonals anti-cytochrome *c* (Pharmingen, San Jose, CA, U.S.A.), anti-Hsp90 (Transduction Laboratories, San Jose, CA, U.S.A.), anti-Hsp27, and anti-Hsp-70 (Stressgen, Victoria, BC, Canada), and polyclonals anti-HSF1 antibody (Stressgen), anti-NF-κB (Santa Cruz Biotechnology, Santa Cruz, CA, U.S.A.), anti-phospho-NF-κB (Cell Signaling Technology, New England BioLabs, Beverly, MA, U.S.A.), anti-IκB-α (Upstate Biotechnology, Lake Placid, NY, U.S.A.), anti-Smac/DIABLO, and anti-AIF (Biomol Research Laboratories, Plymouth Meeting, PA, U.S.A.).

Carbonylated proteins were detected using the Oxyblot Kit (Intergen Company, Purchase, NY, U.S.A.). In brief, 20 μg of proteins was reacted with 2,4-dinitrophenylhydrazine (DNP) for 15 min at 25°C. Samples were resolved on 12% SDS-polyacrylamide gels, and DNP-derivatized proteins were identified by immunoblot using an anti-DNP antibody.

Densitometric analyses of protein bands were performed by the Software Gel Pro Analyzer.

Data are presented as a representative immunoblot of three giving similar results.

Measurement of proteasome activity

Cells were lysed in 100 m*M* HEPES, 10% sucrose, and 0.1% CHAPS. Then 50 μl of lysates was incubated for 30 min at 37°C in 150 μl of 5 m*M* $MgCl_2$, 50 m*M* Tris-HCl, pH 7.8, 20 m*M* KCl, 5 m*M* magnesium acetate, 10 m*M* dithiothreitol. Specific proteasome substrate Suc-LLVY-AMC (Calbiochem–Novabiochem Corp., La Jolla, CA, U.S.A.), which detects chymotrypsin-like activity of proteasome, was added at 50 μ*M*. The reaction was stopped by addition of 200 μl of cold ethanol. The cleavage of substrate was monitored fluorimetrically using a PerkinElmer luminescence spectrometer LS-5 at 460 nm (excitation at 380 nm). Data are expressed as arbitrary units of fluorescence per milligram of proteins.

Immunoprecipitation

Three hundred micrograms of protein was incubated in lysis buffer with 10 μl of polyclonal anti-HSF1 antibody to a total volume of 300 μl for 2 h at 4°C. Immunocomplexes were adsorbed with 20 μl of protein A-Sepharose for 30 min at 4°C. After three washes with lysis buffer, immune pellets were boiled in SDS sample buffer. Fifty microliters of proteins was loaded on 15% SDS-polyacrylamide gel and transferred to nitrocellulose. Monoclonal anti-Hsp90 antibody was used as primary antibody (1:10,000).

Proteins were determined by the method of Lowry *et al.* (21).

Data presentation

Data are expressed as means ± SD, and significance was assessed by Student's *t* test. Differences with p values <0.05 were considered significant.

RESULTS

Cytochrome c *release and apoptosis are not linked events upon GSH depletion*

Cytochrome *c* release from mitochondria represents one of the most important events in response to stress-mediated apoptosis that allow apoptosome formation and caspase activation (5). A redox-mediated mechanism for keeping this protein in the mitochondrial intermembrane space has been suggested, as alterations in the GSH redox state induce both cytochrome *c* release and a rapid induction of the apoptotic mitochondrial pathway (14). However, chemical depletion of GSH does not necessarily result in cell death, implying not a straightforward correlation between the two processes (16). We studied the effects of GSH depletion in promonocytic U937 cells upon treatment with BSO, a specific inhibitor of GSH synthesis. Total cell lysates or cytosolic and mitochondrial fractions were prepared and used for analyses of GSH content by HPLC and cytochrome *c* protein level by western blotting. Figure 1A shows that 1 m*M* BSO induced a time-dependent decrease of GSH up to 12 h of treatment, which became under the limit of detection at 24 h (data not shown). Moreover, the decrease observed influenced the cytosolic as well as the mitochondrial pool, whereas the nuclear-enriched fraction seemed to be less susceptible (Fig. 1B). A concomitant transient release of cytochrome *c* into the cytosol was also observed. Its immunoreactive band became detectable in the cytosolic fraction following 1 h of treatment, peaked between 3 and 6 h, and slowly declined to basal levels over 12 h (Fig. 1C). To determine whether cytochrome *c* release was di-

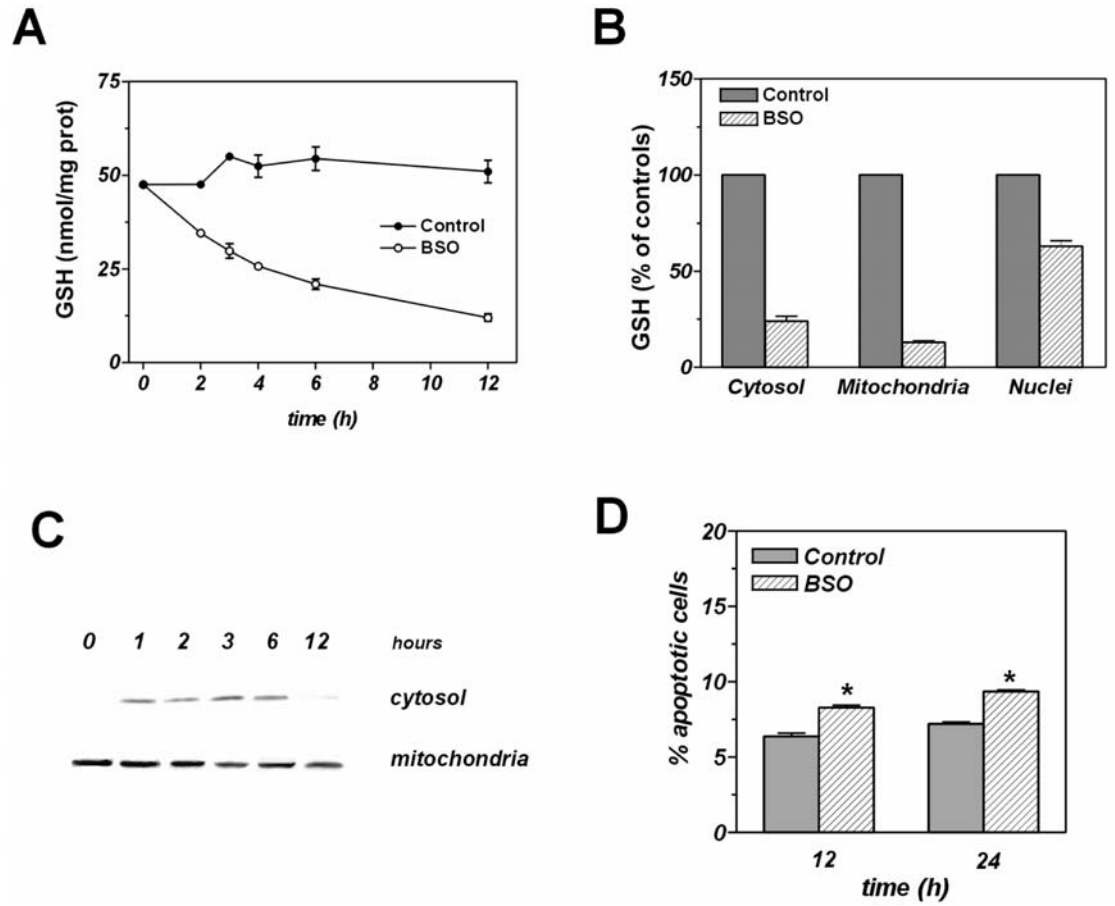

FIG. 1. GSH depletion causes a transient release of cytochrome *c* and a recoverable apoptotic cell death. (A) U937 cells were treated with 1 m*M* BSO. Intracellular GSH content was measured in total cell lysates by HPLC. Data are expressed as means ± SD ($n = 6$). **(B)** U937 cells were treated for 4 h with 1 m*M* BSO. GSH content was measured in cytosolic, mitochondrial, and nuclear fractions by HPLC. Data are expressed as means ± SD ($n = 3$). **(C)** Cytochrome *c* protein levels were determined after treatment with 1 m*M* BSO by immunoblot analysis using a monoclonal antibody. Either 5 μg of proteins from mitochondrial or 25 μg from cytosolic fractions was loaded. Immunoblot is from one experiment representative of three that gave similar results. **(D)** U937 cells were treated with 1 m*M* BSO for 12 or 24 h. Apoptotic cells were detected by cytofluorimetric analysis upon staining with propidium iodide. Data are expressed as means ± SD ($n = 5$). *$p < 0.01$.

rectly associated with induction of apoptosis, we performed cytofluorimetric analyses of cell nuclei stained with propidium iodide. Results shown in Fig. 1D illustrate the percentage of apoptotic U937 cells (hypodiploid nuclei) upon treatment with 1 m*M* BSO. In particular, whereas a slight cytotoxic effect was observed upon 12 h of treatment, as evidenced by the rise in the commitment of cells to apoptosis (+30% of apoptotic population with respect to the values assessed in control cells), longer incubations (24 h) showed no further increase in the percentage of dead cells. Moreover, total cell population was not significantly affected by BSO treatment at both 24 and 48 h (data not shown). These results indicated that the induction of apoptosis was not time-dependent and, at the same time, suggested the existence of efficient repairing mechanisms activated by cells able to abolish the induction of apoptosis downstream of cytochrome *c* release, even under non-physiological oxidant conditions.

BSO-mediated GSH decrease induces nuclear translocation of AIF

The induction of apoptosis via the mitochondrial pathway is a complex process that does not necessarily involve changes in the expression level of specific proteins, but rather implicates the translocation of a few proteins between mitochondria and cytosol, where cytochrome *c* release represents the first step in the apoptosome formation and caspase activation. To assess whether BSO treatment induced changes in the localization of proapoptotic proteins involved in the activation of the mitochondrial pathway other than cytochrome *c*, we performed western blot analyses of cellular fractions. Figure 2 shows Smac/DIABLO and AIF expression levels in mitochondria, cytosol, and/or nuclei, according to the compartment in which the proteins act to induce apoptosis. Treatment with 1 m*M* BSO did not affect the distribution of Smac/DIABLO,

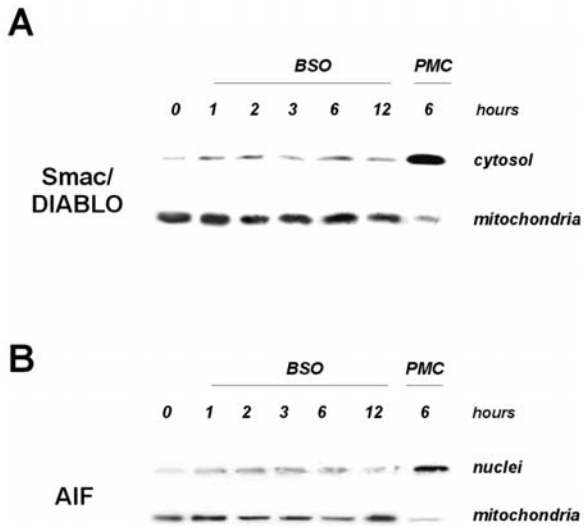

FIG. 2. GSH depletion induces the translocation of AIF. U937 cells were treated at different time points with 1 m*M* BSO. Smac/Diablo **(A)** and AIF **(B)** protein levels were determined by immunoblot analysis using polyclonal antibodies. Twenty-five micrograms of proteins from mitochondrial, nuclear, or cytosolic fractions was loaded. The figure also reports the data obtained upon treatment with 10 μ*M* puromycin (PMC) for 6 h, as positive control. Immunoblots are from one experiment representative of two that gave similar results.

as the intensities of the immunoreactive bands remained unchanged during the time points analyzed (Fig. 2A), whereas a rapid translocation of AIF in the nuclear compartment was observed (Fig. 2B). Moreover, the kinetics of AIF translocation mirrors the cytochrome *c* release into the cytosol; in fact, at 12 h, we observed the recovery of AIF into the mitochondrial compartment. These results suggest that GSH depletion was able to induce both release of cytochrome *c* into the cytosol and AIF nuclear translocation, but did not influence localization of Smac/DIABLO. Figure 2 also reports the levels of Smac/DIABLO and AIF after treatment with 10 μ*M* puromycin, used as positive control, because it has been previously reported that this compound is an efficient apoptotic inducer in U937 cells (15). After 6 h of treatment, a significant translocation of Smac/DIABLO and AIF from the mitochondria into the cytosol and nucleus, respectively, was observed. These results were in agreement with cytofluorimetric analyses of apoptotic cells that accounted for 67.5% of the total cell population (data not shown).

GSH depletion induces mitochondria-specific oxidative insult and proteasome activation

Mitochondria represent the main source of ROS that under physiological conditions accounted for 2% of the electrons transported along the mitochondrial chain. Antioxidant enzymes and GSH are present in these organelles to counteract the damaging effects of ROS. Under BSO treatment, the significant decline in mitochondrial GSH content and the release of cytochrome *c* into the cytosolic compartment suggests a potential harmful condition for these organelles in terms of ROS production. To test this hypothesis, we treated U937 cells with the peroxide- and hydroxyl radical-sensitive fluorophore DHR 123 and assayed ROS level by cytofluorimetric analyses. Figure 3A shows that U937 cells treated with 1 m*M* BSO were subjected to a higher flux of ROS than untreated cells; this increase was significantly different from controls starting from 6 h and reaching the maximum level at 12 h of treatment. However, analyses performed after 24 h showed that fluorescence of BSO-treated cells was superimposable on that of control cells (Fig. 3A).

Proteins could represent a specific target of ROS insult resulting in the oxidation of specific residues and in increase in carbonyl content (3). Cytosolic and mitochondrial extracts were derivatized with DNP and electrophoresed on 10% SDS-polyacrylamide gel. Figure 3B shows a typical ladder of carbonylated proteins of the mitochondrial fraction evidenced by western blot analyses. A time-dependent increase of carbonyl immunoreactive bands during the first 12 h was detected (+35%), whereas no difference could be observed after 24 h of BSO treatment. On the other hand, cytosolic extracts from BSO-treated cells did not exhibit any significant difference in the intensity of the immunoreactive bands with respect to control values (data not shown), indicating a more specific oxidative insult for mitochondria during GSH loss.

Under stress conditions, such as increased production of ROS, which are able to alter protein structure and function irreversibly, cell survival is often assured by the capability of cells to clear damaged proteins by the activity of proteasome machinery. Figure 3C shows that proteasome chymotrypsin-like activity was significantly induced upon treatment with 1 m*M* BSO as soon as 3–6 h after drug addition (+30%) and slowly decreased during the following 24 h.

Hsps and NF-κB systems are activated during cell response to BSO-mediated GSH loss

The data obtained so far indicated that the potentially harmful effects due to GSH depletion did not result in cell death, suggesting a possible induction of defense mechanisms able to inhibit the apoptotic machinery downstream of cytochrome *c* release and/or ROS production. It has been proposed that Hsp27 and Hsp70 are able to counteract apoptosis by binding cytochrome *c* and Apaf1, thus inactivating apoptosome formation (4, 30). To test whether the Hsp system was operative also in our experimental model, thus representing a putative buffer response to cytochrome *c* release from mitochondria, we performed western blot analyses of proteins involved in this process, starting from the upstream Hsp transcription factor HSF1. Figure 4A shows a typical immunoblot of U937 nuclear extracts during the first 12 h of treatment with 1 m*M* BSO. GSH depletion was able to activate the heat shock response by transiently increasing the presence of the phosphorylated isoform of HSF1 within the nuclear compartment, letting us hypothesize an increase in downstream gene transcription. This transcription factor is physiologically present as a dephosphorylated and inactive protein due to inhibitory binding of Hsp70 and Hsp90. To be functionally active, HSF1 has to dissociate from the inhibitory subunits, phosphorylate, trimerize, and translocate into the nucleus, where it acts as inducer of heat shock gene transcription (25). After BSO treatment, total cell lysates

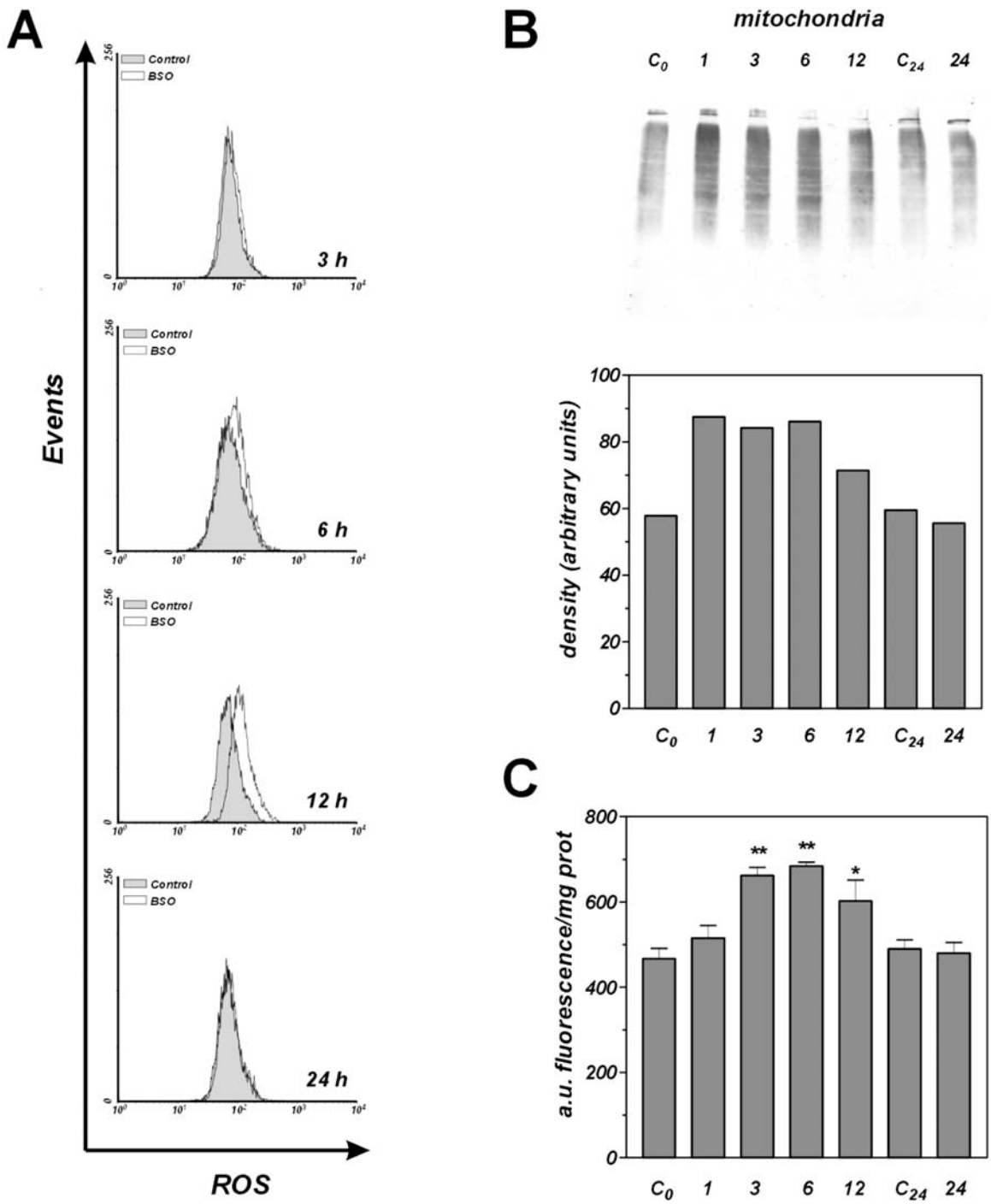

FIG. 3. GSH depletion results in oxidative imbalance and proteasome activation. (A) U937 cells were treated at different time points with 1 m*M* BSO. Intracellular ROS concentration was detected by cytofluorimetric analysis after 30-min incubation with 5 μ*M* DHR 123. Histograms derived from a representative experiment of four that gave similar results are shown. **(B)** Protein carbonyls of mitochondrial fractions were identified upon derivatization with DNP, followed by immunoelectrophoresis using a polyclonal anti-DNP antibody. Twenty micrograms of proteins was loaded onto each lane. Immunoblot is from one experiment representative of three that gave similar results. **(C)** Chymotrypsin-like activity of proteasome was determined by following the cleavage of the fluorogenic substrate Suc-LLVY-AMC. Data are expressed as means ± SD ($n = 6$). *$p < 0.01$; **$p < 0.001$.

were immunoprecipitated with an antibody against HSF1, and the Hsp90/HSF1 heterocomplex was measured by performing western blot analyses with an antibody anti-Hsp90. Figure 4A shows a time-dependent decrease of the Hsp90-immunoreactive band during the time points analyzed, suggesting that dissociation between the two proteins occurred upon BSO treatment. Once activated, HSF1 induces Hsp27 and Hsp70 gene transcription, which results in the increase of the expression

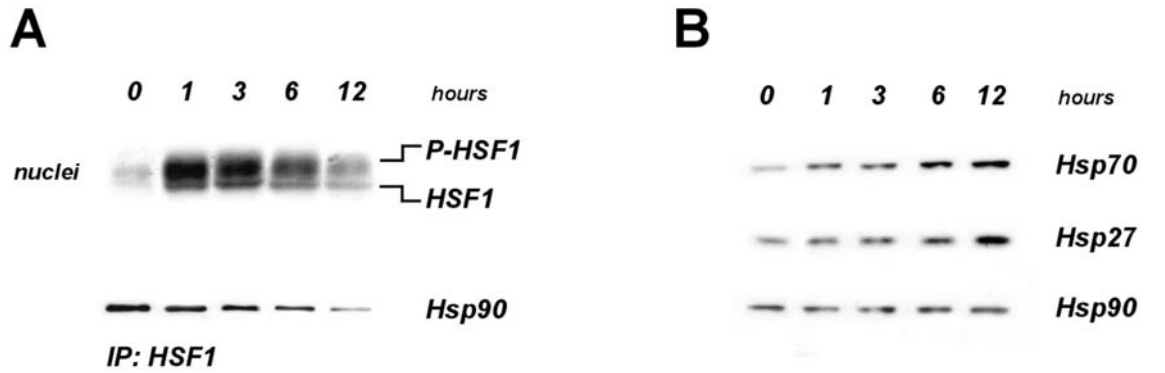

FIG. 4. GSH depletion induces the activation of Hsp system. (A) U937 cells were treated at different time points with 1 m*M* BSO. HSF1 protein levels were detected by immunoblot analysis using a polyclonal antibody. Twenty-five micrograms of protein from nuclear fractions was loaded onto each lane **(upper panel)** (P-HSF1: phosphorylated isoform). Three hundred micrograms of total protein extracts was incubated with an anti-HSF1 polyclonal antibody, and 50 μl of immunoprecipitates was applied onto each lane. Hsp90/HSF1 heterocomplexes were detected by immunoblot analysis with a monoclonal anti-Hsp90 antibody **(bottom panel)**. **(B)** Hsp27, Hsp70, and Hsp90 protein levels were detected by immunoblot analysis using monoclonal antibodies. Ten micrograms of total protein extracts was loaded onto each lane. Immunoblots are from one experiment representative of three that gave similar results.

levels of these two proteins. Under our experimental conditions, this process also occurred as western blot analyses of total cell lysates showed a time-dependent increase of Hsp27 and Hsp70 (Fig. 4B), whereas Hsp90-immunoreactive bands remained unchanged during the time points observed.

It has been suggested that Hsp could also inhibit apoptosis by facilitating the induction of survival proteins (13). One of these proteins is NF-κB, whose several steps of activation involve proteolytic degradation of regulatory proteins. Hsp27 seems to facilitate phosphorylated and ubiquitylated IκB-α proteolytic degradation (24); therefore, we measured the expression levels of IκB-α upon BSO treatment. Figure 5A shows that IκB-α expression level significantly decreases in total lysates. This event was also associated with a concomitant appearance of NF-κB-immunoreactive bands in the nuclear fraction starting from 1 h after BSO treatment (Fig. 5B). The activation of NF-κB was nicely supported by the evidence of a simultaneous increase in the level of its phosphorylated isoform in the nuclear fraction. This result could explain the recovery of cell survival upon the earlier induction of cell death.

BSO triggers apoptosis in cells that are not able to induce Hsp-mediated response

BSO treatment was associated with apoptosis in various cell lineages different from U937 (2, 12). We used leukemia CEM cells to investigate the differences of cell response to GSH depletion with respect to the resistant U937 cells. As shown in Fig. 6A, upon BSO treatment, CEM cells underwent a very rapid decrease in intracellular GSH levels, reaching 65.5% decrement after 1 h. Cytofluorimetric analyses of hypodiploid nuclei stained with propidium iodide evidenced an increase in apoptosis percentage starting from 12 h (12%) and reaching values close to 30% of the total population after 24 h of treatment with 1 m*M* BSO (Fig. 6B).

To correlate cell death to an alteration in the buffer response observed in U937 cells, we performed western blot analyses of Hsp27 and Hsp70. As shown in Fig. 6C, whereas Hsp70 expression levels did not significantly change during 12 h of treatment with BSO, Hsp27 rapidly decreased, suggesting that not only was an antiapoptotic response to GSH depletion not induced, but also the activation of Hsp transcription was selectively inhibited.

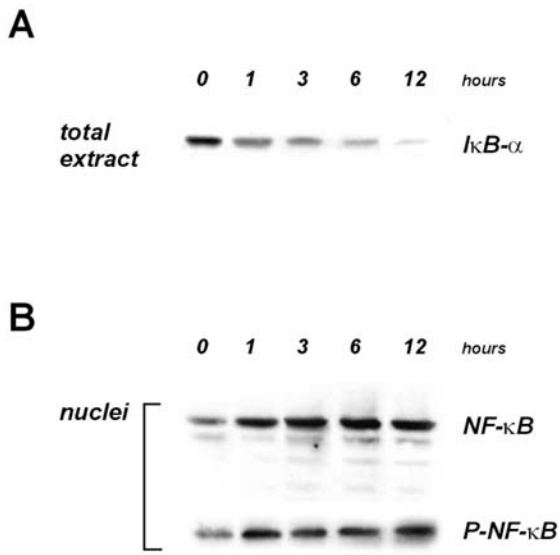

FIG. 5. GSH depletion induces activation of NF-κB. (A) U937 cells were treated at different time points with 1 m*M* BSO. IκB-α protein levels were detected by immunoblot analysis using a polyclonal antibody. Twenty-five micrograms of total protein extracts was loaded onto each lane. **(B)** U937 cells were treated at different time points with 1 m*M* BSO. NF-κB protein levels were detected by immunoblot analysis using a polyclonal antibody. Twenty-five micrograms of protein from nuclear fractions was loaded onto each lane. Immunoblots are from one experiment representative of three that gave similar results.

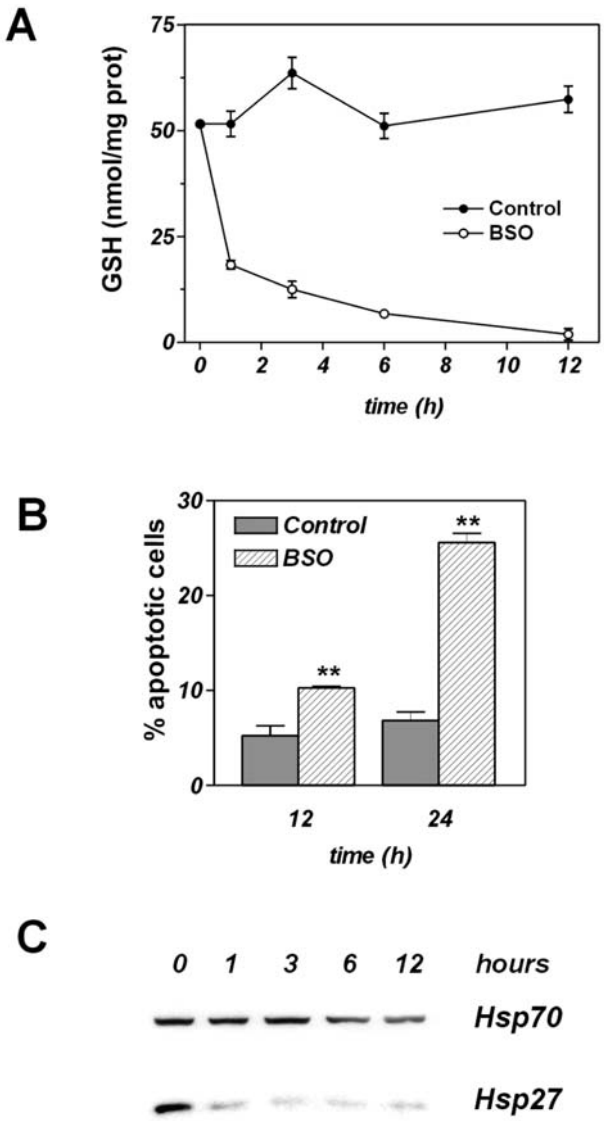

FIG. 6. GSH depletion induces cell death and Hsp down-regulation in CEM cells. (A) CEM cells were treated at different time points with 1 m*M* BSO. Intracellular GSH content was measured on total cell lysates by HPLC. Data are expressed as means ± SD ($n = 6$). **(B)** CEM cells were treated with 1 m*M* BSO at 6, 12, and 24 h. Apoptotic cells were detected by cytofluorimetric analysis upon staining with propidium iodide. Data are expressed as means ± SD ($n = 5$). $^{**}p < 0.001$. **(C)** Hsp27 and Hsp70 protein levels were detected by immunoblot analysis using monoclonal antibodies. Ten micrograms of total protein extracts was loaded onto each lane. Immunoblot is from one experiment representative of three that gave similar results.

DISCUSSION

Apoptotic cell death is triggered by extrinsic receptor-mediated and intrinsic mitochondria-mediated signaling pathways. Moreover, depending on cell type, the receptor-mediated pathway recruits the mitochondrial death machinery in order to allow apoptosis (7); therefore, mitochondria are considered to play a central role in the execution of the cell death program. The release of cytochrome *c* from mitochondria is a critical early event in the mechanism of apoptosis, allowing apoptosome formation and caspase activation (5). Different mechanisms have been postulated to concur in determining this event; however, the entire process(es) remains elusive. An additional intriguing aspect is that referring to the capability of GSH to modulate the localization of cytochrome *c*, depending on its concentration and/or redox state (16, 18). In fact, the occurrence of a massive extrusion of GSH from the intracellular compartment into the extracellular medium is also a well established early event during the phases characterizing cell death commitment (14). However, in several experimental systems, in the absence of specific death stimuli, the depletion of GSH alone was not able to mediate the activation of the apoptotic program. On the other hand, we previously demonstrated that this process was sufficient to induce the release of cytochrome *c* from the mitochondrial intermembrane space (16). Therefore, the results reported in this article, obtained with promonocytic U937 cells, although in line with our previous data, highlight the mechanisms by which cells counteract oxidative stress due to GSH depletion, allowing survival even in the presence of cytosolic cytochrome *c*. Here we demonstrated that BSO induces a time-dependent decrease of GSH and, at the same time, cytochrome *c* is released from mitochondria as soon as 1 h after treatment. Moreover, cytochrome *c* release was associated with AIF nuclear translocation, but not related to Smac/DIABLO relocalization. Therefore, we hypothesize that cytochrome *c* release and AIF translocation could proceed through different modalities: one occurs in response to GSH depletion and could be restored by cells; the other may rely on the pore-forming property of proapoptotic members of the Bcl-X_L family proteins in the presence of apoptotic inducers. As a result of the oxidative imbalance, we observed a mild increase in the apoptotic cell population after 12 h of BSO treatment. This increase was very low compared with the total cell population (7.21% versus 5.20% of untreated cells), but significantly different (+30%) with respect to the apoptotic cells. The most important aspect was the result obtained at 24 h after BSO treatment, where we did not determine a further increase in apoptotic cells, still being +30% of the apoptotic population. On the other hand, total cell number at this time point was similar between control and BSO-treated cells. These data, together with the temporary presence of cytochrome *c* within the cytosol and AIF in the nucleus, suggest the induction of cellular systems able to clear these potentially harmful proteins in order to inhibit their further release and, at the same time, to recover and/or induce cell proliferation.

Furthermore, as a result of the redox imbalance, due to GSH depletion, we observed an increase in ROS and, particularly in the mitochondrial fraction, protein oxidation—phenomena that, again, were also rapidly counteracted by cells. In fact, we observed a complete recover of both protein carbonyls and ROS increase 24 h after treatment. It is noteworthy to point out that GSH at this time point was under the detection limit; thus, the repairing systems were operative under extremely oxidant conditions. Among the cytoprotective systems that could be activated by oxidative stress, Hsps represent a well established example. Under our experimental conditions, we evidenced a rapid activation of the transcription

factor HSF1 and the induction of the expression of its downstream factors Hsp27 and Hsp70. The presence of the active isoform of HSF1 in nuclear extracts and the time-dependent dissociation from its inhibitory partner Hsp90 are evidence that strongly suggest a rapid activation of Hsp response. Induction of Hsp27 and Hsp70 nicely explains the recovery of cell death, as recent observations have demonstrated that these proteins can inhibit apoptosis by various distinct mechanisms (24). In particular, Hsp27 could increase the antioxidant defense of cells by decreasing ROS content and neutralizing the toxic effect of oxidized proteins (28); it prevents the formation of apoptosome by directly sequestering cytochrome *c* once released into the cytosol (4). In addition, it has been reported that Hsp70 prevents the AIF-induced chromatin condensation of purified nuclei, as well as protects cells from the apoptogenic effects of AIF targeted to the extramitochondrial compartment (30). The capability of Hsp70 to interact and recruit Apaf1 in order to prevent apoptosome oligomerization has also been demonstrated. All these antiapoptotic functions could be used under our experimental conditions and could explain, at least in part, the efficient recovery of cell death.

Another survival system that could be activated by oxidant condition is represented by the proteasome, the major proteolytic system involved in the degradation of the oxidatively damaged proteins. This finding correlates with our results; in fact, we determined an increase in the proteasome activity as soon as 3 h after BSO treatment. This increase was still significant after 12 h and declined to the basal level at 24 h. This trend correlates with the cleared oxidized proteins and let us hypothesize an additional role for Hsp27 in assisting cytosolic cytochrome *c* degradation by proteasome. Indeed, the disappearance of cytosolic cytochrome *c* observed after 12 h, without a further induction of apoptosis, might be explained by a selective elimination of the heme protein through the proteolytic action of proteasome.

The conclusions thus far discussed indicate that cells respond to redox change due to GSH loss through at least two distinct pathways: (a) they may buffer cytochrome *c* release and AIF nuclear translocation by rapidly inducing the Hsp system, which efficiently could counteract both the caspase-mediated and the caspase-independent apoptosis; and (b) they may activate proteasome machinery in order to eliminate oxidatively damaged proteins and, most probably, cytosolic cytochrome *c*. We could speculate that, under oxidative conditions, the absence of a real apoptotic stimulus is able to shift the proteolytic cell response from a *widespread* action, which completely destroys cell structures (apoptosis), to a proteasome-mediated *selective* action, which is involved in cell clearance of damaged or unwanted proteins (survival). Proteasome induction could also represent the trigger of other survival responses activated by the cell to counteract oxidative changes upon GSH depletion. In fact, it has been proposed that proteasome can degrade IκB-α, thus letting NF-κB be free to pass the nuclear membrane and activate transcription of survival genes (21). NF-κB seems to be activated in our system after BSO treatment, as demonstrated by the rapid nuclear translocation of the p65 subunit and degradation of the inhibitory partner IκB-α. Furthermore, activation of NF-κB could explain the recovery of cell proliferation observed after 24 h of treatment with BSO and can be strictly related to Hsp induction. In fact, it has been demonstrated that Hsp27 facilitates IκB-α degradation by the proteasome system (24).

Another important aspect of GSH-mediated apoptosis is that cells do not always survive BSO treatment, but often they are induced to death. It has been reported that several cell lines treated with BSO are committed to cell death with the features of apoptosis (2, 12). In this report, we also demonstrated that T-cell leukemia CEM cells underwent apoptosis after BSO challenge. The apoptotic cell population was 12% after 12 h of treatment and proportionally increased with time, reaching a value close to 30% at 24 h. We observed that BSO treatment in these cells was more effective, as GSH decrement was more rapid (after 1 h of treatment, a 64.5% decrement in CEM cells versus 18.2% in U937 cells was determined). This higher rate of GSH depletion might explain, at least in part, the different downstream cell responses. The Hsp system was not induced in these cells, but rather a decrease in the expression levels of both Hsp27 and Hsp70 was determined. This result suggests the role played by these proteins in the survival of U937 cells, but, we are not able to explain the different responses of the two cell lines to BSO treatment. Work is in progress in our laboratory to assess if the rate of GSH depletion could make the difference. We also suggest that cell type could be an important factor in this network, at least in the case of U937 cells. They derived from monocytes where GSH is fundamental also for the phagocytic processes. It has been demonstrated that, during phagocytosis, GSH content decreased by 80% during the first 2 h of the process with a concomitant increase of the tripeptide in the extracellular environment (29). Therefore, macrophagic cells could be well equipped against GSH loss. Whether cytochrome *c* is released during phagocytosis is currently under evaluation in our laboratory.

ACKNOWLEDGMENTS

This work was partially supported by grants from FIRB, CNR, MIUR, and Ministero della Sanità—"Progetto di Ricerca Finalizzata."

ABBREVIATIONS

AIF, apoptosis-inducing factor; Apaf1, apoptosis protease-activating factor 1; BSO, buthionine sulfoximine; DHR 123, dihydrorhodamine 123; DIABLO, direct IAP-binding protein with low pI; DNP, 2,4-dinitrophenylhydrazine; GSH, glutathione; GSSG, glutathione disulfide; HSF, heat shock factor; Hsp, heat shock protein; IAP, inhibitors of apoptotic proteins; NF-κB, nuclear factor-κB; PBS, phosphate-buffered saline; ROS, reactive oxygen species; SDS, sodium dodecyl sulfate; Smac, second mitochondria-derived activator of caspases.

REFERENCES

1. Adrain C and Martin SJ. The mitochondrial apoptosome: a killer unleashed by the cytochrome seas. *Trends Biochem Sci* 26: 390–397, 2001.
2. Anderson CP, Tsai JM, Meek WE, Liu RM, Tang Y, Forman HJ, and Reynolds CP. Depletion of glutathione by buthionine sulfoximine is cytotoxic for human neuroblas-

toma cell lines via apoptosis. *Exp Cell Res* 246: 183–192, 1999.
3. Aquilano K, Rotilio G, and Ciriolo MR. Proteasome activation and nNOS down-regulation in neuroblastoma cells expressing a Cu,Zn superoxide dismutase mutant involved in familial ALS. *J Neurochem* 85: 1324–1335, 2003.
4. Bruey JM, Ducasse C, Bonniaud P, Ravagnan L, Susin SA, Diaz-Latoud C, Gurbuxani S, Arrigo AP, Kroemer G, Solary E, and Garrido C. Hsp27 negatively regulates cell death by interacting with cytochrome *c*. *Nat Cell Biol* 2: 645–652, 2000.
5. Cain K, Bratton SB, and Cohen GM. The Apaf-1 apoptosome: a large caspase-activating complex. *Biochimie* 84: 203–214, 2002.
6. Cande C, Cohen I, Daugas E, Ravagnan L, Larochette N, Zamzami N, and Kroemer G. Apoptosis-inducing factor (AIF): a novel caspase-independent death effector released from mitochondria. *Biochimie* 84: 215–222, 2002.
7. Esposti MD. The roles of Bid. *Apoptosis* 7: 433–440, 2002.
8. Filomeni G, Rotilio G, and Ciriolo MR. Cell signalling and the glutathione redox system. *Biochem Pharmacol* 64: 1057–1064, 2002.
9. Filomeni G, Rotilio G, and Ciriolo MR. Glutathione disulfide induces apoptosis in U937 cells by a redox-mediated p38 MAP kinase pathway. *FASEB J* 17: 64–66, 2003.
10. Flohè L. Glutathione peroxidase: fact and fiction *Ciba Found Symp* 65: 95–122, 1978.
11. Franklin CC, Krejsa CM, Pierce RH, White CC, Fausto N, and Kavanagh TJ. Caspase-3-dependent cleavage of the glutamate-L-cysteine ligase catalytic subunit during apoptotic cell death. *Am J Pathol* 160: 1887–1894, 2002.
12. Friesen C, Kiess Y, and Debatin KM. A critical role of glutathione in determining apoptosis sensitivity and resistance in leukemia cells. *Cell Death Differ* 11 Suppl 1: S73–S85, 2004.
13. Garrido C, Gurbuxani S, Ravagnan L, and Kroemer G. Heat shock proteins: endogenous modulators of apoptotic cell death. *Biochem Biophys Res Commun* 286: 433–442, 2001.
14. Ghibelli L, Coppola S, Rotilio G, Lafavia E, Maresca V, and Ciriolo MR. Non-oxidative loss of glutathione in apoptosis via GSH extrusion. *Biochem Biophys Res Commun* 216: 313–320, 1995.
15. Ghibelli L, Fanelli C, Rotilio G, Lafavia E, Coppola S, Colussi C, Civitareale P, and Ciriolo MR. Rescue of cells from apoptosis by inhibition of active GSH extrusion. *FASEB J* 12: 479–486, 1998.
16. Ghibelli L, Coppola S, Fanelli C, Rotilio G, Civitareale P, Scovassi AI, and Ciriolo MR. Glutathione depletion causes cytochrome *c* release even in the absence of cell commitment to apoptosis. *FASEB J* 13: 2031–2036, 1999.
17. Ghosh S and Karin M. Missing pieces in the NF-κB puzzle. *Cell* 109: S81–S96, 2002.
18. Iverson SL and Orrenius S. The cardiolipin–cytochrome *c* interaction and the mitochondrial regulation of apoptosis. *Arch Biochem Biophys* 423: 37–46, 2004.
19. Lee MH, Hyun DH, Marshall KA, Ellerby LM, Bredesen DE, Jenne P, and Halliwell B. Effect of overexpression of Bcl-2 on cellular oxidative damage, nitric oxide production, antioxidant defences and the proteasome. *Free Radic Biol Med* 31: 1550–1559, 2001.
20. Lewis J, Devin A, Miller A, Lin Y, Rodriguez Y, Neckers L, and Liu ZG. Disruption of hsp90 function results in degradation of the death domain kinase, receptor-interacting protein (RIP), and blockage of tumor necrosis factor-induced nuclear factor-kappaB activation. *J Biol Chem* 275: 10519–10526, 2000.
21. Lowry OH, Rosebrough NJ, Farr AL, and Randall RJ. Protein measurement with the Folin phenol reagent. *J Biol Chem* 193: 265–275, 1951.
22. Mattson MP and Kroemer G. Mitochondria in cell death: novel targets for neuroprotection and cardioprotection. *Trends Mol Med* 9: 196–205, 2003.
23. Nicoletti I, Migliorati G, Pagliacci MC, Grignani F, and Riccardi C. A rapid and simple method for measuring thymocyte apoptosis by propidium iodide staining and flow cytometry. *J Immunol Methods* 139: 271–279, 1991.
24. Parcellier A, Gurbuxani S, Schmitt E, Solary E, and Garrido C. Heat shock proteins, cellular chaperones that modulate mitochondrial cell death pathways. *Biochem Biophys Res Commun* 304: 505–512, 2003.
25. Pirkkala L, Nykanen P, and Sistonen L. Roles of the heat shock transcription factors in regulation of the heat shock response and beyond. *FASEB J* 15: 1118–1131, 2001.
26. Ravagnan L, Gurbuxani S, Susin SA, Maisse C, Daugas E, Zamzami N, Mak T, Jaattela M, Penninger JM, Garrido C, and Kroemer G. Heat-shock protein 70 antagonizes apoptosis-inducing factor. *Nat Cell Biol* 3: 839–843, 2001.
27. Reed DJ, Babson JR, Beatty PW, Brodie AE, Ellis WW, and Potter DW. High-performance liquid chromatography analysis of nanomole levels of glutathione, glutathione disulfide, and related thiols and disulfides. *Anal Biochem* 106: 55–62, 1980.
28. Rogalla T, Ehrnsperger M, Preville X, Kotlyarov A, Lutsch G, Ducasse C, Paul C, Wieske M, Arrigo AP, Buchner J, and Gaestel M. Regulation of Hsp27 oligomerization, chaperone function, and protective activity against oxidative stress/tumor necrosis factor alpha by phosphorylation. *J Biol Chem* 274: 18947–18956, 1999.
29. Rouzer CA, Scott WA, Griffith OW, Hamill AL, and Cohn ZA. Glutathione metabolism in resting and phagocytizing peritoneal macrophages. *J Biol Chem* 257: 2002–2008, 1982.
30. Saleh A, Srinivasula SM, Balkir L, Robbins PD, and Alnemri ES. Negative regulation of the Apaf-1 apoptosome by Hsp70. *Nat Cell Biol* 2: 476–483, 2000.
31. Thornberry NA and Lazebnik Y. Caspases: enemies within. *Science* 281: 1312–1316, 1998.

Address reprint requests to:
Maria Rosa Ciriolo, Ph.D.
Department of Biology
University of Rome "Tor Vergata"
Via della Ricerca Scientifica, 1
00133 Rome, Italy

E-mail: ciriolo@bio.uniroma2.it

Received for publication February, 26, 2004; accepted October 17, 2004.